Rotational motion in thermally excited nuclei

S. Leoni and A. Bracco

4. Rotational motion in thermally excited nuclei*

4.1. Introduction

The study of the nucleus at the limits of excitation energy and angular momentum is one of the central topics addressed with EUROBALL γ-spectroscopy measurements. In particular, the study of the rotational motion at finite temperature plays a crucial role in the understanding of the properties of the nuclear system beyond the mean field description, providing relevant information on the two-body residual interaction responsible for the band-mixing process.

At present, we know that, in medium mass nuclei, already at few hundreds keV excitation energy above the yrast line, rotational bands are close enough in energy to interact by residual interactions. This implies that the shell-model states occurring at low excitation energy will mix strongly, leading to complicated stationary states that no longer correspond to any simple motion, as a part of the general order-to-chaos transition that the nucleus undertakes with increasing temperature. As a consequence, due to the different response of the intrinsic states to the Coriolis and centrifugal forces, the rotational motion becomes *damped*, namely the electric quadrupole decay from a single state at spin I will be distributed over a spectrum of final states all at spin I-2, with a strength function whose width at half maximum is called the *rotational damping width* Γ_{rot} [117]. This results in quasi-continuum ridge-valley structures in γ–coincidence spectra, which are not accessible by standard discrete spectroscopy techniques. The dependence of the rotational damping width on the mass number A, the nuclear shape deformation ε, the angular momentum I and the intrinsic excitation energy U of the nucleus has been originally predicted by a schematic model [117], and lately confirmed by more realistic calculations [118].

In the last two decades considerable experimental effort has been given to the study of the rotational motion at finite temperature. Focusing on nuclei of mass A~160 the gross features have been explored in a long series of pre-EUROBALL experiments, making use of smaller arrays such as NORDBALL, GASP, EUROGAM I and II. By making use of an ad-hoc technique based on a statistical analysis of γ–γ and higher fold coincidences, it was for the first time possible to extract quantitative information from the quasi-continuum distributions [119]. In fact, the very existence of a *finite* number of γ-decay paths, below the particle binding energy, leads to enhanced fluctuations in γ-coincidence spectra (at variance from a purely statistical spectrum), whose magnitude is fixed by the number of paths. In addition, the development of cranked shell model calculations, including a two-body residual interaction allowed for a proper direct comparison between data and theory [118].

The first basic result obtained with the fluctuation analysis technique has been the direct experimental evidence for the damping phenomenon [120], earlier studied via comparison of the spectrum landscape with simulation calculations of the γ-decaying cascades only [121]. In this context, the importance of the two-body residual interaction has also been established in the onset of the damping phenomenon and in the further transition to the compound nucleus regime at higher excitation energies. The basic features of the residual interaction, such as its intensity and its dependence on the various component of the two-body force, have also been established by a comparison with experimental data concerning the number of discrete unresolved bands [118,122]. The dependence of rotational damping on the intrinsic nuclear

* Contribution by S. Leoni and A. Bracco

configuration, corresponding for example to specific values of the K quantum number (e.g. high-K vs. low-K) has also been investigated to establish the degree of mixing of the various configuration in the gradual transition towards the compound nucleus regime [123]. A review of these achievements obtained in the field of warm rotation can be found in Ref. [124].

In more recent years, the study of rotational damping has been focused on the dependence on nuclear mass and deformation. This has been done making use of high statistics EUROBALL experiments concerning normal-deformed nuclei in the mass region A~110 and super-deformed nuclei in the mass regions A~140 and 160 as well as in connection with a search for the Giant Dipole Resonance built on highly deformed nuclei, as it will be discussed in the following sections.

From the discussion presented in the following it is clear that the extensive work made so far has indeed allowed to make a good progress in the understanding of the structure of warm nuclei. However, as discussed in the final section, there are still basic questions which are not fully solved, mainly related to the precise determination of the rotational and compound nucleus widths [125], and to the direct experimental observation of the GDR on superdeformed nuclei.

4.2. Mass dependence of rotational damping

One of the main achievements in the field of warm rotation, obtained with EUROBALL experiments, has been the study of the dependence of the damping phenomenon on the nuclear mass and deformation. As originally proposed in a schematic formulation of the damping model [117], the energy U_0 for the onset of rotational damping and the rotational damping width Γ_{rot} are expected to depend on the level density and on the strength of the

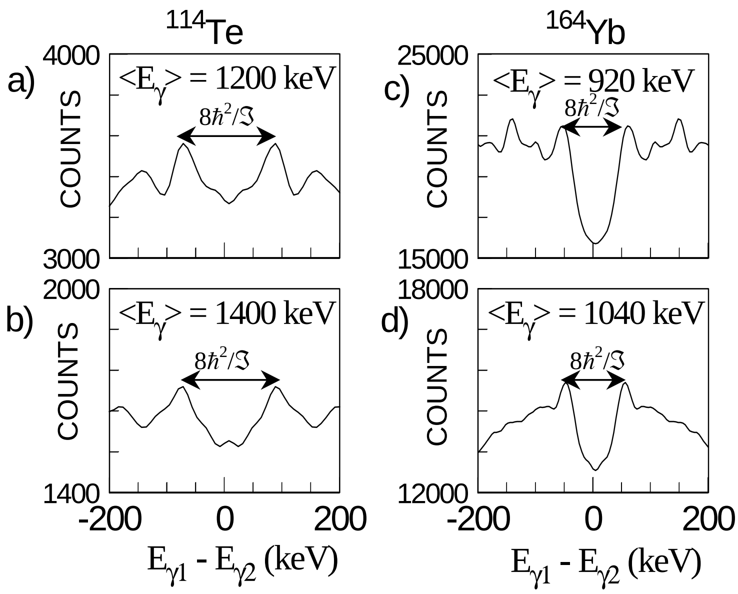

Figure 4.1: *Perpendicular cuts on γ-γ coincidence matrices of ^{114}Te and ^{164}Yb at the average transition energy indicated in each panel. The separation between the two most inner ridges (indicated by arrows in the figure) can be directly related to the moment of inertia of the rotating nucleus (adapted from Ref. [126]).*

two-body residual interaction, leading to the dependences $U_0 \propto A^{-2/3}$ and $\Gamma_{rot} \propto I\, A^{-5/2}\, \varepsilon^{-1}$, with I and ε being the spin and the nuclear deformation, respectively.

The validity of the relations given above has been established by the study of nuclei with similar deformation (ε~0.25), but with different masses, namely ^{164}Yb (A~160) and ^{114}Te (A~110). As discussed in Ref. [126], the analysis has been performed on quasi-continuum spectra, which in both cases are characterised by similar rotational pattern, forming ridge-valley structures in γ–γ coincidence matrices, as shown in Figure 4.1. In particular, while the ridges are populated by unresolved discrete excited bands extending up to the onset of rotational damping, the valley region collects the contribution from the warmer region of damped rotation.

Figure 4.2 (a) shows the results obtained from the fluctuation analysis of the ridge structures observed in the γ–γ coincidence spectra of ^{114}Te and ^{164}Yb, as reported in Ref. [126]. It is found that the number of paths is of the order of 25 for the typical rare earth nucleus ^{164}Yb, while it is smaller by approximately a factor of 2 in the ^{114}Te case, as it was also observed in the case of ^{112}Sn in the same mass region [127]. The solid lines in the figure represent the theoretical value for the number of discrete excited bands populating the ridge structures, as obtained from band-mixing calculations for the rare earth nucleus ^{168}Yb and for ^{114}Te [118]. It is found that the calculations, averaged over the spin interval 25-35ℏ, well reproduce the experimental data.

As shown in Figure 4.2 (b), the number of damped decay paths, obtained from the analysis of the valley region, is found to be much larger (of the order of 10^3-10^4), again with a significant difference between the ^{114}Te and ^{164}Yb data. The full drawn lines give the expected theoretical dependence obtained by applying the fluctuation analysis technique to numerically calculated spectra produced by the simulation code MONTESTELLA [128], which are based on calculated levels and transition probabilities for a specific nucleus, as obtained by the same band-mixing calculations used for the analysis of the ridge structures. As one sees from the figure, the calculations are found to reproduce both the ridge and the valley results quite well, giving a strong support to the band-mixing model in different regions of masses [118].

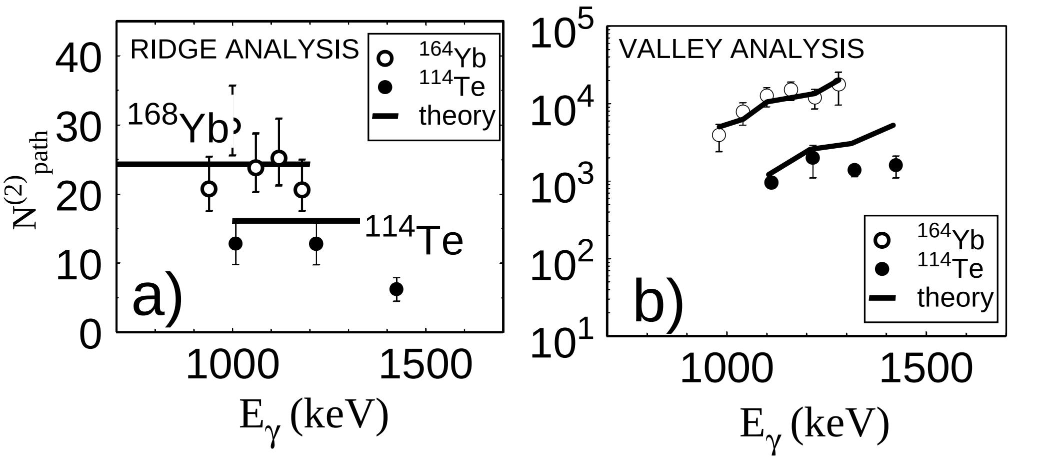

Figure 4.2: *The number of decay paths $N^{(2)}_{path}$ extracted from γ–γ coincidence matrices of ^{164}Yb and ^{114}Te by a fluctuation analysis of the first ridge (panel a) and valley (panel b). The solid lines give the theoretical predictions from the band-mixing model of ref. [118] (adapted from Ref. [126]).*

The quantitative agreement between calculations and experiment, seen in Figure 4.2, strongly supports the scaling with mass number of the residual interaction and of the level density. According to the present band-mixing calculations, damping should set in around a heat energy of $U_0 \sim 0.9$-1.0 MeV in ^{114}Te, compared with $U_0 \sim 0.7$-0.8 MeV in ^{168}Yb, in rather good agreement with the scaling $U_0 \propto A^{-2/3}$, originally proposed in Ref. [117].

An experimental estimate of the upper limit of the rotational damping width Γ_{rot} can be inferred by measuring the width of the E2 bump constructed as a difference between single spectra at consecutive bombarding energies, as discussed in Ref. [126,127]. In such cases, since all the decays from the entry distribution contribute to the difference spectrum, and not only E2 transitions corresponding to a given $I \rightarrow I-2$ decay, the widths of the difference spectra can only be taken as an upper limit for the rotational damping width. The results obtained from such an analysis are given in Figure 4.3, where the damping width Γ_{rot} measured in the normal-deformed nuclues ^{114}Te and in the superdeformed nucleus ^{143}Eu is given relative to the corresponding value in ^{164}Yb [124]. As can be seen from the figure, consistency is found among all evaluations, supporting the dependence of the rotational damping width Γ_{rot} on the mass A, nuclear shape deformation ε and spin I, as originally predicted [117]. However, only the scaling of Γ_{rot} has been measured, but not yet the absolute value of the rotational damping width. One may conclude that the dependence of the damping mechanism on the mass and deformation can be closely tested by studying the shapes and fluctuations carried by γ-coincidence spectra produced by excited rotating nuclei.

4.3. Superdeformation at finite temperature

In recent years, weakly populated structures of superdeformed nature, corresponding to highly elongated prolate nuclear shapes with an approximate axis ratio of 2:1, have been found in many different mass regions [14] (cf. Section 1). This has motivated many theoretical and experimental investigations, mainly aiming at the understanding of the mechanisms which allow to observe these peculiar configurations over a wide spin interval, from the fission limit down to the angular momentum region where the superdeformed yrast band rather suddenly decays into the normal-deformed states. We now know that this is due to the presence of different nuclear shapes (normal and superdeformed), which can coexist over a wide spin range, being well separated by a potential energy barrier in the deformation space. The tunneling through the potential energy barrier allows the decay-out of the superdeformed states into the normal-deformed states (cf. Section 3).

This scenario has been extensively investigated in the case of the superdeformed yrast and of the first few superdeformed excited bands experimentally observed, while much less information is available on the thermally excited rotational motion in the superdeformed well. This is because it requires not only the experimental analysis of quasi-continuum spectra connected with the superdeformed structures, but also the comparison with calculations describing both the thermally excited rotational motion and the barrier penetration effect.

The superdeformed quasi-continuum has been extensively studied in the nucleus ^{143}Eu, during a series of pre-EUROBALL and EUROBALL experiments [96,97,129]. In this case, ridge structures with a spacing corresponding to the moment of inertia of the superdeformed yrast line have been observed in the high transition energy region of γ–γ coincidence matrices, and for the first time a lifetime analysis based on the measurement of the fractional Doppler shift of the ridges has been performed [97]. As shown in Figure 4.4, the fractional Doppler shift

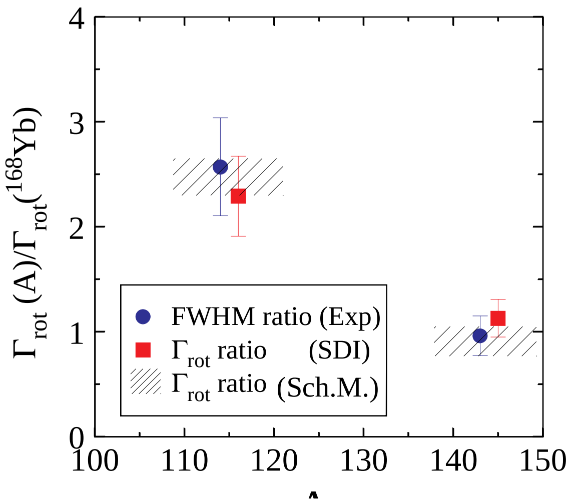

Figure 4.3: *The scaling of the damping width Γ_{rot} with the mass number A, the deformation parameter ε and the spin I, is tested for the normal deformed (ND) nucleus ^{114}Te and for the SD nucleus ^{143}Eu, with respect to the ND nucleus ^{164}Yb.The full circles correspond to the experimental values, the full squares to the microscopic band mixing predictions, while the dashed areas give the expected ratio according to the simple estimate $\Gamma_{rot} \propto I\ A^{-5/2}\ \varepsilon^{-1}$ of the schematic model of Ref. [117] (from Ref. [124]).*

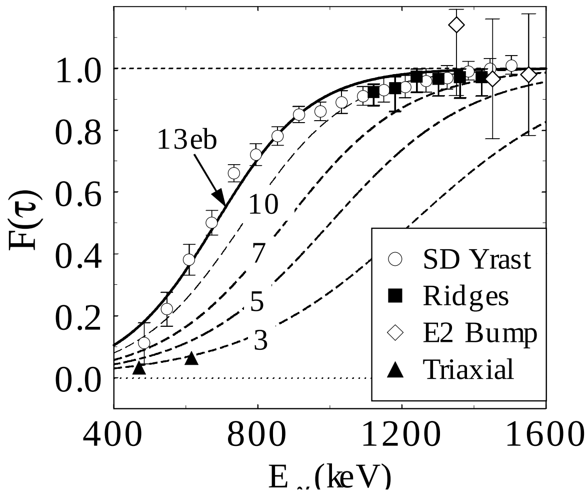

Figure 4.4: *Fractional Doppler shifts as measured for the SD yrast (circles), the SD ridges (squares), the E2 collective bump (diamonds) and the triaxial transitions (triangles) observed in the nucleus ^{143}Eu. The curves represent the theoretical $F(\tau)$ values for quadrupole moments of Q_t = 3, 5, 7, 10 and 13 eb (from Ref. [97,124]).*

F(τ) measured for the ridge structures (squares) is consistent with a quadrupole moment of 10-13 eb, as obtained from the analysis of the superdeformed yrast band of ^{143}Eu, giving further support to the superdeformed nature of the unresolved discrete excited bands populating the ridges.

The superdeformed ridge structures observed in the γ–γ coincidence matrices of ^{143}Eu have been further investigated by the statistical analysis of the counts fluctuations [119,97]. This has allowed to estimate the total number of discrete (excited) superdeformed rotational bands, which can not be resolved individually due to their extremely weak population. As shown in Figure 4.5, it is found that the number of superdeformed excited discrete bands depends very strongly on the transition energy, reaching a constant value of ~30 at the highest energies, where the superdeformed ridge structure is populated. In contrast, at lower transition energies the number of superdeformed bands is found to decrease continuously, while the intensity of the ridge structure is still observed to increase. The experimental results have been compared with microscopic cranked shell model (CSM) calculation plus a two-body residual interaction for the specific nucleus ^{143}Eu [130,99]. It is found that the predicted number of discrete excited superdeformed bands reproduces the experimental data at the maximum of the distribution, while it deviates strongly at lower transition energies. This is generally expected for the lower part of the ridge structure, as a consequence of the barrier penetration into the first well.

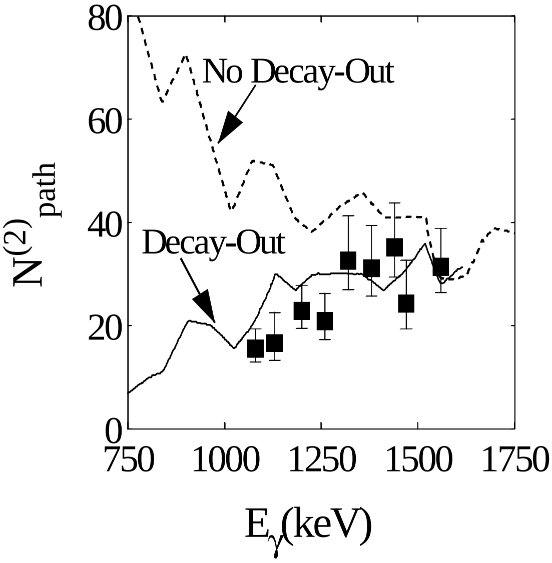

Figure 4.5: *Number of excited rotational bands extracted from the analysis of the superdeformed ridges of ^{143}Eu (squares), compared with CSM calculations including a two-body residual interaction (broken curve) [99]. The solid line represents the theoretical predictions including the decay-out process into the normal-deformed well [97].*

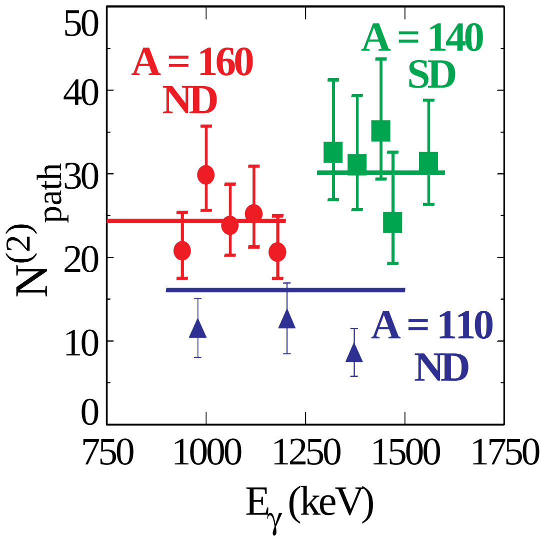

Figure 4.6: *Number of decay paths $N^{(2)}_{path}$ extracted from the fluctuation analysis of the first ridge of γ–γ coincidence matrices collecting the γ-decay flow from normal-deformed (ND) nuclei ^{164}Yb (A=160) and ^{114}Te (A=110), and from the superdeformed (SD) nucleus ^{143}Eu (A=140). The solid lines give the theoretical predictions from the band model of Ref. [118,99] (from Ref. [124]).*

The reduction in the measured number of excited superdeformed bands can be reproduced by the model, when the decay-out mechanism of the excited states is taken into account (solid line) [98,131]. In the model, the superdeformed states obtained by cranking calculations are coupled to normal-deformed compound states which lie energetically near, following a prescription similar to the one used in the case of the decay-out of the superdeformed yrast band. In this way, the decay-out of the excited superdeformed states is described in terms of a quantum tunneling through the potential energy barrier in the deformation space, leading some components of the normal-deformed states to be mixed into the superdeformed state. Since the normal-deformed states also have an associated electromagnetic transition probability, the superdeformed state thus mixed will have the possibility of decaying not only with rotational E2 transitions within the superdeformed well, but also with γ rays feeding to the normal states, thereby giving rise to the decay-out into the normal-deformed well.

One can then conclude that the satisfactory agreement between the data and the number of superdeformed bands predicted by the microscopic calculations, including also the decay-out mechanism, not only provides a clear evidence for the tunneling process in the thermally excited nucleus, but also gives a further support to the validity of the band-mixing model, which is found to properly describe the thermally excited rotational motion in different regions of mass and deformation. This is clearly illustrated in Figure 4.6 where the number of superdeformed bands of ^{143}Eu, measured in the transition energy region not affected by the decay-out process (e.g. 1300 keV < E_γ < 1600 keV) is compared with the band-mixing model predictions, together with similar results for normal-deformed nuclei of mass A~110 and 160.

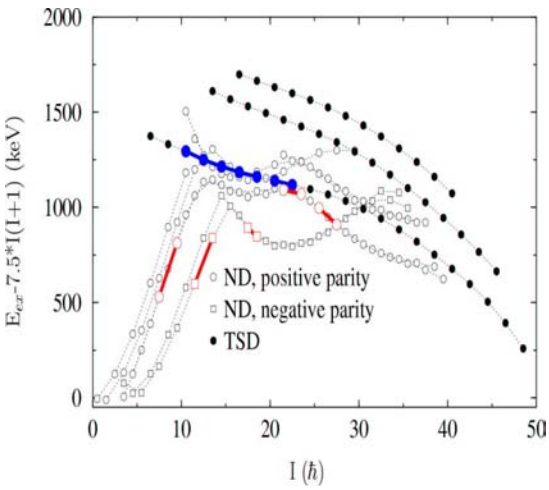

Figure 4.7: *Excitation energy relative to a rigid rotor for selected normal deformed (ND) and triaxial superdeformed (TSD) bands in ^{163}Lu. The transitions used for creating the gated matrices are marked by a solid line together with larger symbols for the initial and final states [90].*

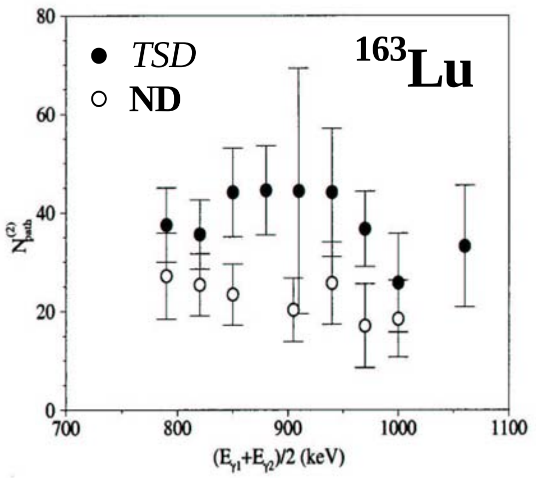

Figure 4.8: *Number of two-step paths along the TSD ridge of ^{163}Lu, as obtained from the fluctuation analysis of the TSD gated matrix (filled circles) and ND gated matrix (open circles) [90].*

The triaxial superdeformed nucleus ^{163}Lu has also offered the possibility to study the excited rotational motion in a strongly deformed well. According to theoretical predictions based on the modified oscillator potential, local minima in the potential energy surface are expected at deformation $\varepsilon \sim 0.4$, with a triaxiality parameter $\gamma \sim \pm 20^{o}$. These predictions have been recently confirmed in a series of EUROBALL experiments (cf. Section 2), by the observation of one and two-phonon excitations, which are the first firm experimental evidence for a stable triaxial deformation in nuclei [58,60].

The properties of this nucleus at excitation energies above the energies of the resolved triaxial superdeformed discrete bands have been investigated by a fluctuation analysis [90]. In order to study the onset of damping in this triaxial superdeformed nucleus and to learn more about the mixing mechanisms between excited triaxial superdeformed states and normal-deformed states, γ–γ coincidence matrices gated by normal-deformed (ND) and TSD yrast transitions have been constructed. In particular, as shown in Figure 4.7, the transitions used as ND gates have been carefully selected in order to avoid any contaminants from the strongly populated TSD band, which is observed to decay-out into the normal-deformed well at lower spins as compared to the ND gates.

It is found that a similar ridge structure, with a spacing corresponding to the moment of inertia of the TSD yrast band, is present in both γ–γ coincidence matrices gated by ND and TSD configurations, although no sign of the strongly populated TSD yrast is observed in the ND gated matrix. Figure 4.8 shows the number of discrete unresolved bands populating the TSD ridge, obtained by the fluctuation analysis of the TSD and ND gated matrices. While for the TSD ridge the average number of bands is ≈ 40, the number of paths extracted from the ND gated matrix is almost a factor of 2 lower.

In order to explain these experimental findings, it has been suggested that about fifty percent of the TSD paths feed into the normal-deformed potential well, due to a mixing between the unresolved states in the two minima at excitation energies right below the onset of damping, but still above a certain energy U_M, where mixing sets in and induces a cross-talk between the potential wells. As schematically illustrated in Figure 4.9, at lower excitation energy, the potential barrier is most probably too large, and the bands closer to the TSD yrast states stay in the TSD well. Therefore, when they finally decay into the normal-deformed well it happens at such a lower angular momentum that the decay cascades bypass the ND gates used. Alternatively, the observed types of decay-paths may not originate from the same states, and this possibility could be investigated by a covariance analysis on experimental data with a better statistics [132].

Figure 4.9: *Schematic illustration of the two potential wells in ^{163}Lu. While U_0 indicates the onset energy of rotational damping, U_M indicates the threshold of mixing between the states in the TSD and ND potentials [90].*

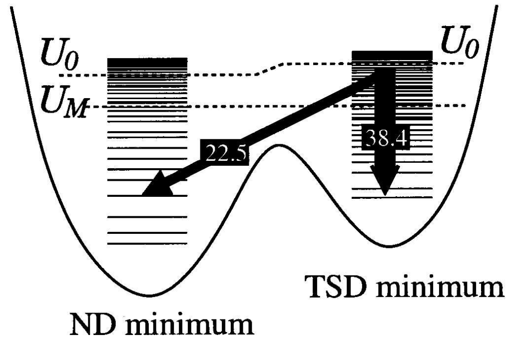

In conclusion, the study of the excited rotational motion in the superdeformed well is found to provide valuable information on the mixing between normal and superdeformed states, leading to the tunnelling process through the potential energy barrier between the two minima. However, several open questions concerning the coupling between the different configurations still remain, calling for better statistics experiments with the next generation of Ge detector arrays.

4.4. Role of E1 feeding in the population of the superdeformed states

The study of the quasi-continuum in the superdeformed nucleus ^{143}Eu has also been an essential tool for the understanding of the feeding mechanism of superdeformed states. In fact, one of the outstanding problems in superdeformation is the understanding of the population of such structures (in particularly the yrast one) which, at the highest spins, are found to be one order of magnitude larger than in normal-deformed nuclei. To explain this finding it has been proposed that the cooling of the residual nucleus by statistical E1 transitions could be an important mechanism leading to the population of the superdeformed states [93]. This is due to both the shape of the giant dipole resonance (GDR) built on a superdeformed configuration (which is expected to display a low-energy component around 8-10 MeV excitation energy above yrast) and to the lower level density of the superdeformed states [133]. Although several attempts have been made in the last decade to find experimental evidence for the E1 feeding of superdeformed states, no conclusive answer could be given to the problem, mainly due to the experimental limitations.

In the ^{143}Eu experiment, previously discussed in connection with the analysis of the rotational quasi-continuum, the EUROBALL array was combined with 8 large-volume BaF_2 scintillation detectors from the HECTOR array, for the measurement of high-energy γ–rays [95]. This made it possible to investigate the effect of the E1 population of the superdeformed states through the γ-decay of the GDR built on a superdeformed nucleus, by measuring the relative intensity of the superdeformed band, of the ridge structure and of the E2 bump at different values of the gating high-energy γ rays. As shown in Figure 4.10, the relative intensities of the superdeformed yrast band (squares), of the superdeformed ridges (triangles) and of the E2 bump (circles) are found to rapidly increase with the high-energy gating transition, following the ratio between the superdeformed GDR strength function and the spherical one (dashed line). This is also consistent with the expected behaviour from simulation calculations of the γ–ray cascades, including the E1 cooling mechanism from the GDR built on a superdeformed nucleus and the mixing process with the normal-deformed states (full drawn line). In contrast, the relative intensities of less-deformed configurations also observed in ^{143}Eu (represented by the open symbols) do not show any sensitivity to the high-energy condition. One may conclude that the enhanced feeding of the superdeformed structures consistently shows the important role played by the E1 emission from the GDR built on superdeformed states in the population of such highly deformed shapes.

Figure 4.10: *Intensity of the superdeformed yrast band (squares), superdeformed ridges (triangles) and E2 bump (circles) of ^{143}Eu, as function of the high-energy gating transition (normalized at 3 MeV). Similar values for spherical and triaxial deformed transitions are given by open symbols. The dashed and full drawn lines represent the ratio of the superdeformed and normal-deformed GDR strength functions, and the relative intensity of the superdeformed yrast band, respectively, as obtained from more refined simulation calculations, including the E1 cooling mechanism from the superdeformed GDR, and the mixing between normal- and superdeformed states (from [134]).*

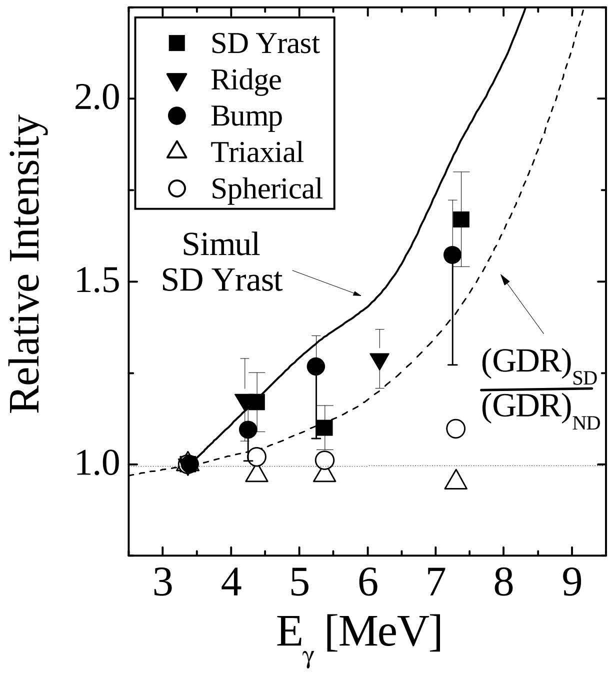

In the same EUROBALL experiment it was also attempted to measure directly the GDR built on the superdeformed configuration. The nucleus ^{143}Eu represents a favourable case in this respect since it shows particular features, which should make the search for the γ-decay of the GDR built on a superdeformed shape more favourable by selecting cascades that populate yrast and excited superdeformed states. In fact, it was found that both the superdeformed yrast band and the excited superdeformed states of the E2 continuum follow decay routes leading to the population of spherical low-spin states only [96]. This is a consequence of the higher potential energy barrier between the superdeformed and the triaxial minimum. This feature of the superdeformed structures of ^{143}Eu can be exploited to search for the γ-decay of the GDR built on superdeformed nuclei in spectra gated by spherical low-spin transitions. In fact, since these transitions collect a large fraction of the entire superdeformed flux (and not

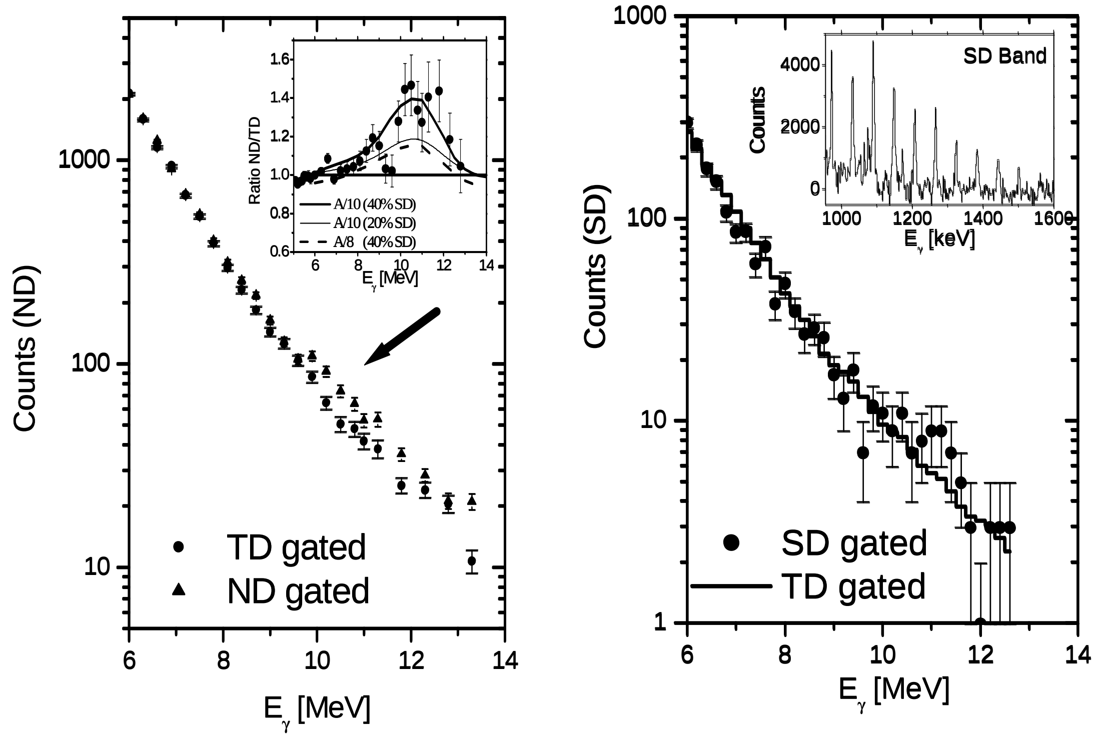

Figure 4.11 (Left panel): *High-energy spectra of* ^{143}Eu *measured with* BaF_2 *detectors, obtained by double-gating on the low-spin spherical transitions (populated by the SD decay, triangles) and on triaxial configuration (not populated by the SD decay, circles). The inset of the figure shows the ratio spectrum obtained by dividing the ND by the TD gated spectrum. The dashed curve uses* $a=A/8$ MeV^{-1} *for the level density parameter of all states, while the solid line curves use the value* $a= A/10$ MeV^{-1} *for the superdeformed states, assuming 40% (thick line) and 20% (thin line) intensity for the superdeformed component.* ***(Right panel):*** *Comparison of a high-energy γ-ray spectrum double gated by the lines of the superdeformed yrast band (filled circles) with the spectrum gated by lines of the triaxial configuration. The inset of the figure shows the spectrum of the superdeformed yrast band measured with Ge detectors in coincidence with γ-rays with* $E_\gamma>3$ *MeV measured in the* BaF_2 *detectors (adapted from [95]).*

only from the yrast band), the high energy γ-ray spectrum gated by these lines should provide a stronger signal than in the spectrum gated by the superdeformed yrast band only.
The left panel of Figure 4.11 shows high-energy spectra measured in the BaF_2 detectors requiring either double gates on spherical (ND) low-spin transitions (populated by the super-deformed flux, triangles) or double gates on triaxial (TD) configurations (*not* populated by the superdeformed states, circles). As shown by the arrow, an excess yield is observed in the ND-gated spectrum in the region 9 – 12 MeV, where one expects to find the low-energy component of the superdeformed Giant Dipole Resonance. This excess can be better seen in the ratio spectrum between the ND- and TD-gated spectra, as shown in the inset of the figure. The intensity excess is found to be rather small (being in average 20%) in agreement with simple statistical model calculations based on a modified version of the CASCADE code (see figure caption for more details).

In the right panel of Figure 4.11 is also shown an attempt to measure the GDR strength function directly gating on the superdeformed yrast band (shown in the inset). As one can see from the figure, in spite of the rather poor statistics of the SD-gated spectrum, one cannot rule out the presence of an excess yield in the same region as observed in the left part of Figure

4.11. Further experimental confirmations are however necessary in other regions of mass, aiming also at a direct gate on superdeformed yrast lines, which will benefit from more powerful Ge detector arrays such as AGATA.

4.5. The double giant resonance in fusion-evaporation reactions

The interest in the study of the double giant resonance state is related to the search of the phonon-phonon interaction and anharmonic effects in nuclear collective modes. A relevant aspect to be investigated is the possible dependence of the anharmonicity on the nuclear temperature and its correlation with the parameters characterizing the double giant dipole resonance (DGDR) state.

The available experimental data about the DGDR are related to the resonance built on the ground state. A way to study temperature effects on this two phonon state is to use fusion-evaporation reactions. However, the first step in this search is a characterisation of the DGDR events which requires the measurement of two coincident high energy γ-rays (with $E_\gamma > 8$ MeV). The emission of two coincident energetic γ-rays has been observed in the reaction ^{37}Cl + ^{120}Sn at the bombarding energy of 187 MeV and using the EUROBALL array [135]. It has been found that the shape of the γ-ray spectrum obtained by requiring a coincidence with a second photon having energy in the range E_γ = 6-20 MeV is roughly accounted by statistical model predictions.

The attribution of events from the decay of the double giant dipole resonance state relies on the fact that the multiplicity of these events is larger than the estimated upper limits for the emission of two uncorrelated photons in the same deexcitation cascade. From these indications obtained with the EUROBALL experiment it is clear that any further investigation on the temperature effects in multi-phonon states requires the use of a detector system with better high-energy response and suppression of neutron events. In addition, an implementation in the statistical model codes of the excitation and decay of the DGDR is necessary for the interpretation of the data.

4.6. Future Perspectives

Important progress has been made in the understanding of the structure of warm nuclei. But in spite of the extensive work carried out in the field of rotational motion at finite temperature, as here discussed in connection with recent EUROBALL experiments, several questions still remain to be addressed. Among them, there is the direct measurement of the spreading width of the B(E2) strength, namely the rotational damping width Γ_{rot}. As discussed in Section 4.1, this quantity appears not easily accessible, since it is experimentally difficult to isolate excited rotational transitions corresponding to a given $I \rightarrow I-2$ decay. However, according to recent theoretical studies based on microscopic band-mixing calculations [125], information on the rotational damping width Γ_{rot}, and also on a much more fundamental quantity such as the compound nucleus width Γ_μ, are expected to be obtained from the analysis of the spectral shape of double and higher fold γ-coincidence spectra. Such kind of studies requires large statistics EUROBALL-type experiments, allowing to select specific intrinsic nuclear configurations.

In connection with superdeformation, a further study of quasi-continuum spectra, based on larger statistics experiment than presently available, is expected to give additional crucial information on the mixing mechanism between excited normal-deformed and superdeformed states, leading to the quantum tunnelling through the potential energy barrier in the deformation space. This is also expected to shed light on the gradual transition from order to chaos undertaken by the nuclear system with increasing temperature.

Moreover, in order to obtain a full understanding of the feeding mechanism of the super-deformed structures from the Giant Dipole Resonance one needs additional work in other mass regions than presently investigated (^{143}Eu), also in connection with particle feeding mechanisms.

Acknowledgements

The reported work stems from a long collaboration within the community of EUROBALL users. In particular, we like to acknowledge G. Benzoni, F. Camera, B. Million, M. Pignanelli, E. Vigezzi from the University of Milano and INFN (Italy), T. Døssing, G. Hagemann, B. Herskind, S. Ødegård from the Niels Bohr Institute of Copenhagen (Denmark), A. Maj, M. Kmiecik from the Niewodniczanski Institute of Nuclear Physics of Crakow (Poland), M. Matsuo from the Graduate School of Science and Technology of Niigata University (Japan), K. Yoshida from the Institute of Nuclear Science of Nara University (Japan) and Y. Shimizu from the Department of Physics of Kyushu University, Fukuoka (Japan).